Increased methane production associated with community shifts towards *Methanocella* in paddy soils with the presence of nanoplastics

Zhibin He[1], Yarong Hou[1], Ying Li[1], Qicheng Bei[2], Xin Li[3], Yong-Guan Zhu[4], Werner Liesack[5], Matthias C. Rillig[6], Jingjing Peng[1]*.

[1]State Key Laboratory of Nutrient Use and Management, College of Resources and Environmental Sciences, National Academy of Agriculture Green Development, Key Laboratory of Plant-Soil Interactions, Ministry of Education, China Agricultural University, Beijing, 100193, China.

[2]Department of Biological Sciences, University of Southern California, Los Angeles, CA, 90089-0371, USA.

[3]Institute of Agricultural and Nutritional Sciences, Martin-Luther-Universität Halle-Wittenberg, Betty-Heimann-Strasse 5, Halle (Saale), Germany.

[4]State Key Laboratory of Urban and Regional Ecology, Research Centre for Eco-Environmental Sciences, Chinese Academy of Sciences, Beijing, 100085, China.

[5]Max Planck Institute for Terrestrial Microbiology, Karl-von-Frisch-Str. 10, Marburg, 35043, Germany.

[6]Institute of Biology, Freie Universität Berlin, Berlin, 14195, Germany.

* Correspondence: jingjing.peng@cau.edu.cn (Jingjing Peng)

Supplementary Figures

Figures S1 to S31

Figures S1 to S31

Fig. S1 Detailed information on the experimental design.

Fig. S2 Dynamics of CH_4 and CO_2 production in response to different concentrations of LDPE NPs over the 160 day-incubation period.

Fig. S3 Scanning electron microscope (SEM) micrographs of LDPE NPs before the NPs particles were used in experimental treatments.

Fig. S4 Changes in the relative composition of DOM molecules in black (a) and red (b) soils between CK and the treatment with 0.5% LDPE nanoplastics. The DOM composition was determined after the 30-day and 160-day incubation periods. The DOM composition is shown according to formula classes and compound groups. CHONS refer to carbon (C), hydrogen (H), oxygen (O), nitrogen (N), and sulfur (S).

Fig. S5 Concentration of short-chain fatty acids in black and red soils. Acetate, propionate, butyrate, valerate, and lactate were determined after the microcosm incubations for 9 days, 30 days, and 160 days.

Fig. S6 Concentration of long-chain fatty acids in black and red soils after the microcosm incubations for 30 days and 160 days.

Fig. S7 The percentage change in net CH_4 production in NPs-amended microcosms of the black and red soils after the 30-day and 160-day incubation periods. The percentage change in net CH_4 production was calculated in relation to the control treatment (CK).

Fig. S8 The percentage change in the *mcrA* gene copy numbers in NPs-amended microcosms of the black and red soils after the 30-day and 160-day incubation periods. The percentage change in *mcrA* gene copy number was calculated in relation to the control treatment (CK).

Fig. S9 Phylogenomic trees showing the taxonomic relatedness of all 391 bacterial and methanogen MAGs. While the taxonomic affiliations of the 353 bacterial MAGs are shown at the phylum level, those of the 38 methanogen MAGs are indicated at the family level. The solid boxes in the most inner circle indicate bacterial and methanogen MAGs whose metagenomic abundance is significantly correlated to DOC (blue boxes)

and CH_4 (red boxes). Three strip charts indicate the completeness, contamination, and GC (%) of each MAG. The asterisk(s) in the most outer circle represent genome size.

Fig. S10 Representative MAGs that were recovered from black and red soils and exhibited significant changes in their metagenomic abundance between the different treatments (CK, 0.5% NPs, and 5% NPs).

Fig. S11 The 20 most abundant bacterial families in the metagenomes of the control (CK) and LDPE NPs treatments (0.5%, 5%) in the black and red soils after the 30-day and 160-day incubation periods.

Fig. S12 The normalized abundance and the taxonomic assignment of H_2-evolving hydrogenase genes in the black soil and red soil metagenomes obtained from the control (CK) and LDPE NPs (0.5%, 5%) treatments after the 30-day and 160-day incubation periods. (a) Letters (a,b,c) indicate significant difference in the metagenomic abundance of the H_2-evolving hydrogenase genes between the treatments. Error bars denote standard deviation (n=3). (b) The taxonomic assignment of the H_2-evolving hydrogenase genes was achieved by extracting their sequences from the metagenomic contigs. The extracted sequences were then blasted against the NCBI's non-redundant protein database using Diamond with default settings.

Fig. S13 Principal coordinate analysis (PCoA) of the genes encoding the degradation of aromatics and complex carbohydrates The PCoAs are based on Bray–Curtis distance matrices.

Fig. S14 Treatment-dependent relationship between DOC content and the metagenomic abundance of genes encoding the degradation of aromatics (red lines) and complex carbohydrates (blue lines) in the black and red soils after the 30-day and 160-day incubation periods. Solid lines indicate significance ($P < 0.05$) of the Pearson's correlations, while dashed lines denote non-significance ($P > 0.05$).

Fig. S15 Change in the metagenomic abundance of genes involved in the degradation of aromatics and complex carbohydrates between the 30-day and 160-day incubation periods. The relative abundance changes between the two incubation times and their

significance is shown for each treatment (CK, 0.5% NP, and 5% NP) and soil type. The abundance changes are indicated in counts per million COGs.

Fig. S16 Treatment-dependent relationship between the *mcrA* gene copy number and the metagenomic abundance of genes encoding the degradation of aromatics (red lines) and complex carbohydrates (blue lines) in black and red soils after the 30-day and 160-day incubation periods. Solid lines indicate significance ($P < 0.05$) of the Pearson's correlations, while dashed lines denote non-significance ($P > 0.05$).

Fig. S17 Treatment-specific relationship between the CH_4 production and the metagenomic abundance of genes encoding the degradation of aromatics and complex carbohydrates in the black and red soils after 30-day incubation. The metagenomic abundance is indicated as counts per million COGs. Solid lines indicate significance ($P < 0.05$) of the Pearson's correlations, and dashed lines denote non-significance ($P > 0.05$).

Fig. S18 The bar plots display the phylum-level assignment of genes encoding the degradation of aromatics and complex carbohydrates. Data represents means of three replicates.

Fig. S19 Circle chart showing the set of genes involved in the degradation of complex carbohydrates and affiliated with bacterial families that, according to LEFse analysis, were specifically enriched in the LDPE nanoplastics treatments (relative to CK) of the black soil or the red soil after the 30-day and 160-day incubation periods. The family-level composition is colored-coded. Circle size is proportional to the relative taxon-specific metagenomic abundance.

Fig. S20 Circle chart showing the set of genes involved in the degradation of aromatics and affiliated with bacterial families that, according to LEFse analysis, were specifically enriched in the LDPE nanoplastics treatments (relative to CK) of the black soil or the red soil after the 30-day and 160-day incubation periods. The family-level composition is colored-coded. Circle size is proportional to the relative taxon-specific metagenomic abundance.

Fig. S21 Heatmap showing the presence of genes encoding particular methanogenic pathways in the 38 methanogen MAGs that were recovered from the LDPE nanoplastics treatments after the 30-day and 160-day incubation periods. The genes and gene clusters represent either common biomarkers for the methanogenic potential or are grouped according to the following pathways: acetoclastic, hydrogenotrophic, and methylotrophic methanogenesis.

Fig. S22 Taxonomic assignment of mRNA that is highly specific for the acetoclastic, hydrogenotrophic, or methylotrophic methanogenesis pathway. The mRNA was obtained from the control and 0.5% NPs treatments of the red soil after the 160-day incubation period. The mRNA analysis is based on a composite sample (n = 3).

Fig. S23 Family-level comparison of metatranscriptomic mRNA obtained from the 0.5% NPs treatments of the black soil (BS) and the red soil (RS) after the 160-day incubation period. The mRNA is grouped according to the following pathways: acetoclastic, hydrogenotrophic, and methylotrophic methanogenesis.

Fig. S24 Metagenomic abundance of genes encoding methanogenesis in the control (CK) and LDPE nanoplastics (0.5%, 5%) treatments of the black and red soils after an incubation period of 30 and 160 days. Schematic presentation of low or high changes in the metagenomic abundance of genes associated with the acetoclastic, hydrogenotrophic, or methylotrophic methanogenesis pathways (left panel). The magnitude of the abundance changes is indicated for each gene across the different treatments by circle size (right panel).

Fig. S25 Collective metagenomic abundance of genes highly indicative of (i) acetoclastic, (ii) hydrogenotrophic, or (iii) methylotrophic methanogenesis in the control (CK) and LDPE nanoplastics (0.5%, 5%) treatments of the black and red soils after the 30-day and 160-day incubation periods. The abundance of common methanogenic marker genes (*mcrA*, *mtr*) is shown separately. (a) The data are shown as relative abundances in the format of a heatmap plot. (b) The data are shown as metagenomic abundances in the format of bar graphs. The collective abundance of

genes highly specific for the three methanogenic pathways, along with the relative abundance of *mcr* and *mtr* genes, was set to 100%.

Fig. S26 Changes in the metagenomic abundance of the *mcr* and *mtr* genes in the control (CK) and LDPE nanoplastics (0.5%, 5%) treatments of the black and red soils after the 30-day and 160-day incubation periods. The bar charts are based on the same datasets as shown in Fig. 6. The cumulative relative abundance of the *mcr* and *mtr* genes, along with the relative abundance of the genes encoding the three methanogenesis pathways as shown in Fig. 6, collectively account for 100%. Error bars denote standard deviation (n = 3). The relative abundance of *mcr* and *mtr* genes was calculated based on counts per million reads.

Fig. S27 Linear relationships between the DOC content and the normalized collective metagenomic abundance of genes (counts per million reads) highly indicative of the acetoclastic, hydrogenotrophic, or methylotrophic pathway in the black and red soils after the 30-day and 160-day incubation periods.

Fig. S28 Metabolic pathways expressed in the five order-level methanogen lineages based on the mapping of metatranscriptomic mRNA to the 38 methanogen MAGs obtained in the course of this study. The expression analysis involved energy conservation and ABC transporter, as well as the carbon, nitrogen, and sulfate metabolism.

Fig. S29 Bar graphs showing the relative pathway-specific abundances of transcripts encoding acetoclastic, hydrogenotrophic, or methylotrophic methanogenesis in the metatranscriptomes obtained from the control and 0.5% NPs treatments of the red soil (RS) after the 160-day incubation period. The analysis involved a mapping-independent (direct) mRNA analysis (a) and a mapping-dependent mRNA analysis using 14 methanogen MAGs. Each metatranscriptome was mapped separately. The relative abundances are indicated as percentage of total reads annotated to KEGG level 3 (methane metabolism).

Fig. S30 The normalized metagenomic abundances of the *almA* and *alkB* genes (counts per million reads) in the control (CK) and LDPE NPs (0.5%, 5%) treatments of the

black and red soils after the 30-day and 160-day incubation periods.

Fig. S31 Correlations between the metagenomic abundance of Syntrophomonadaceae and the concentrations of oleic acid and cis-vaccenic acid across the control (CK) and LDPE NPs (0.5%, 5%) treatments of the black soil after the 30-day and 160-day incubation periods.

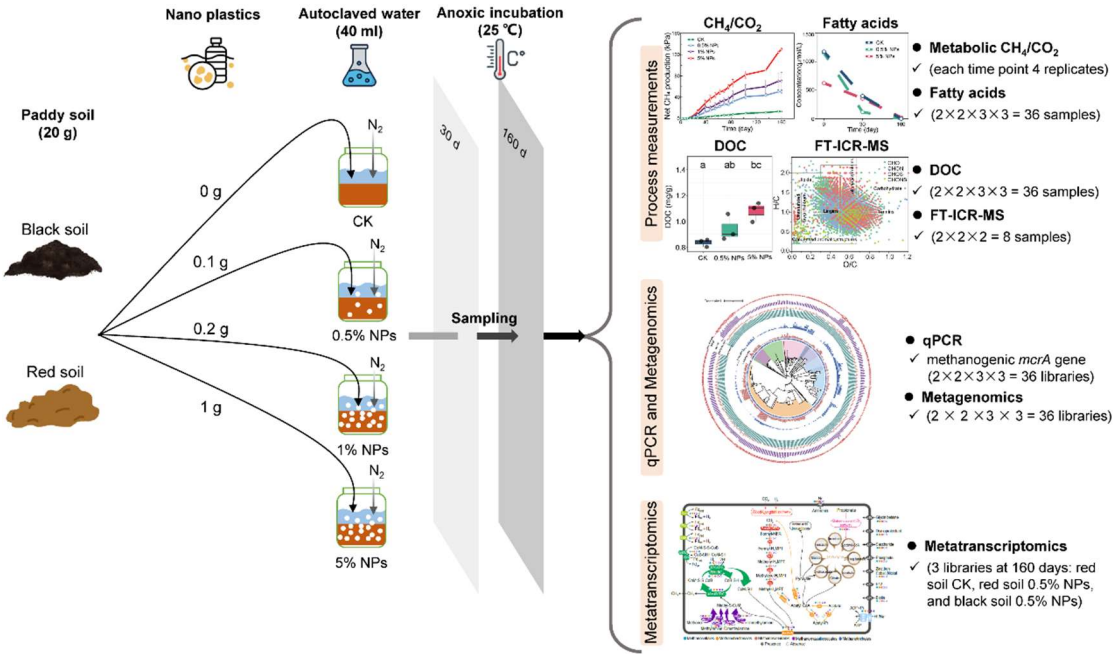

Fig. S1 Detailed information on the experimental design.

Slurry microcosms (20 g dry black soil or red soil, 40 ml autoclaved water, and the appropriate amounts of LDPE nanoplastics [NPs]) were incubated for up to 160 days under anoxic conditions (headspace flushed for 10 min with N_2) at 25°C. All experimental approaches were applied to both soil types, black soil and red soil.

The process measurements involved monitoring the accumulation of CH_4 and CO_2, analysis of volatile fatty acids, as well as the amount and composition of dissolved organic carbon (DOC). Methane and CO_2 were continuously measured over the 160-day incubation period using four replicates for control (CK) and each NP treatment (CK, 0.5%, 1%, and 5%). The microcosm incubations amended with 0.5% and 1% NPs showed similar results. Therefore, three experimental treatments, including CK, 0.5% NPs, and 5% NPs, were selected for downstream analysis.

The measurements of volatile fatty acids (acetate, propionate, valerate, and lactate) and DOC were done in triplicate for each NP treatment (CK, 0.5%, 5%) and time point (30 d, 160 d). The DOC composition for both black and red soils was determined by FT-ICR-MS for the CK and 0.5% NPs treatments at both sampling time points (30 d, 160 d), using composite soil samples of three slurry microcosms.

The molecular analyses involved quantitative PCR (qPCR) of methanogenic *mcrA* genes, metagenomics, and metatranscriptomics. qPCR and metagenomics were done for the three NP treatments (CK, 0.5%, 5%) at both sampling time points (30 d, 160 d) with three biological replicates.

To further substantiate our DNA-based results, we decided to conduct a metatranscriptomic analysis of total RNA (simultaneous analysis of rRNA and mRNA) for CK and 0.5% NPs treatments after an incubation period of 160 days. Composite samples of three microcosms were used for RNA extraction. Despite repeated attempts, the extraction of total RNA of sufficient quality and quantity for library preparation unfortunately failed for the CK treatment of black soil.

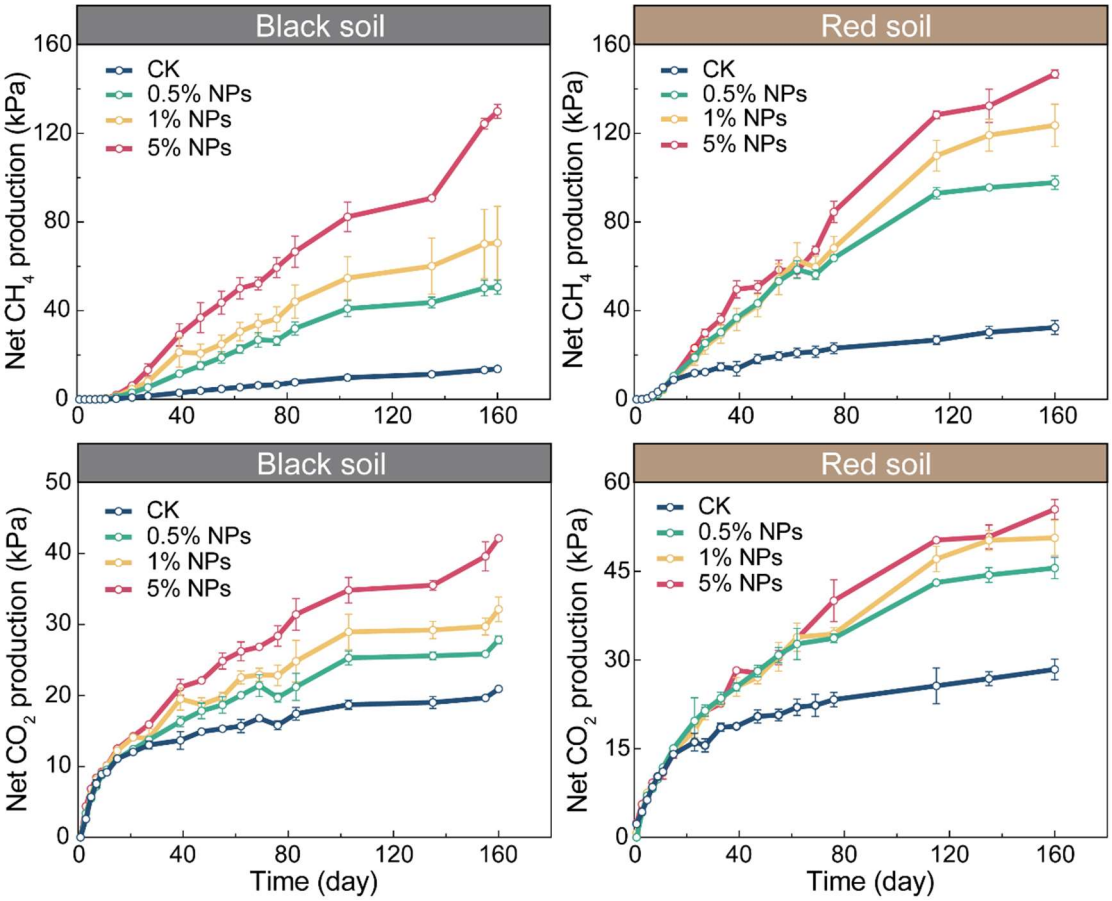

Fig. S2 Dynamics of CH_4 and CO_2 production in response to different concentrations of LDPE NPs over the 160 day-incubation period.

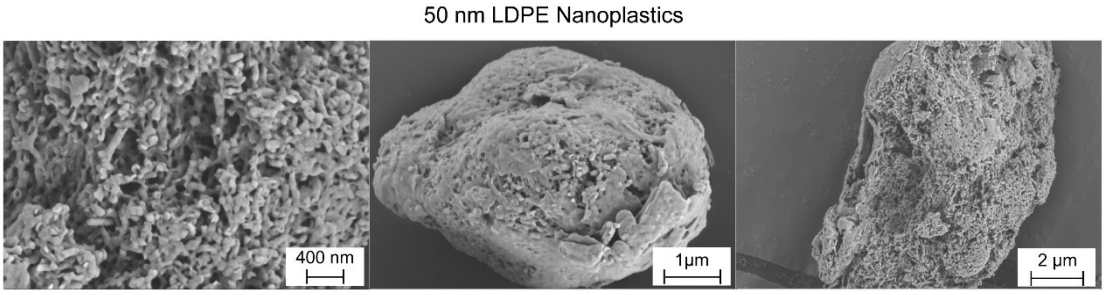

Fig. S3 Scanning electron microscope (SEM) micrographs of LDPE NPs before the NPs particles were used in experimental treatments.

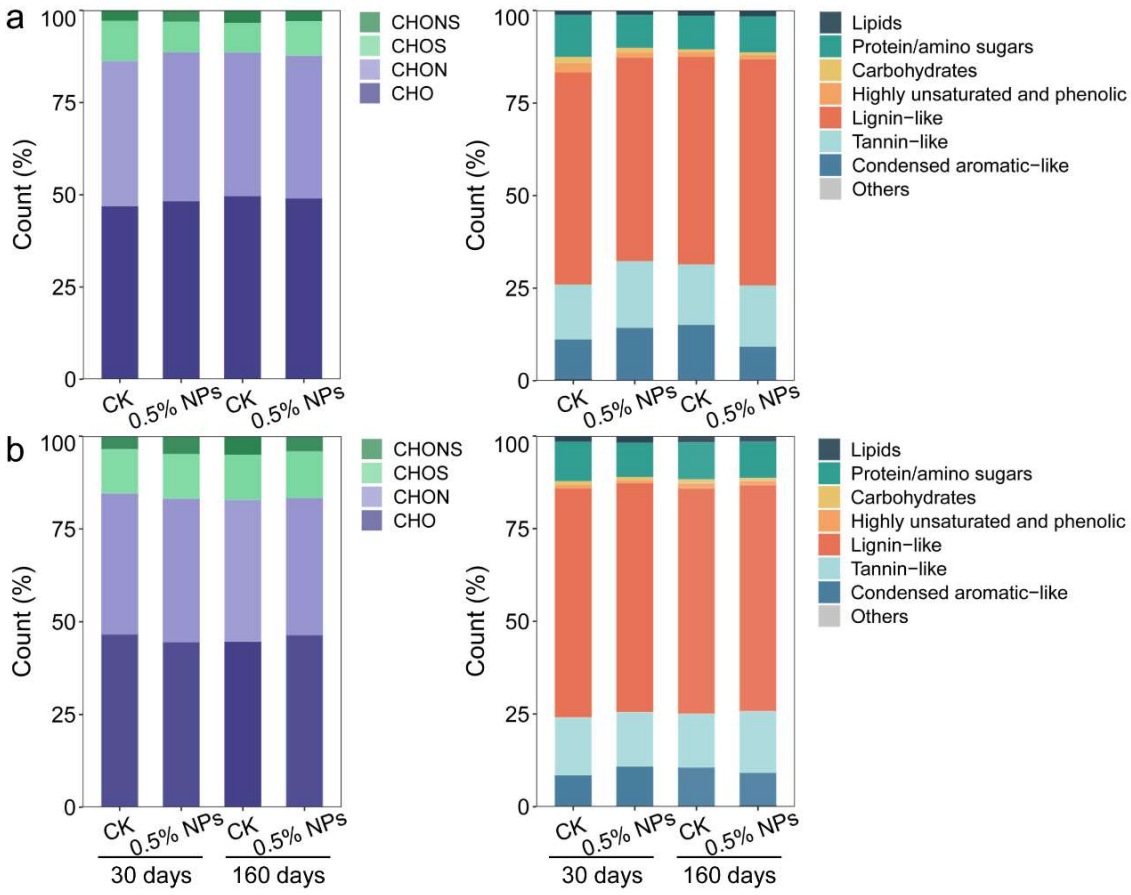

Fig. S4 Changes in the relative composition of DOM molecules in black (a) and red (b) soils between CK and the treatment with 0.5% LDPE nanoplastics. The DOM composition was determined after the 30-day and 160-day incubation periods. The DOM composition is shown according to formula classes and compound groups. CHONS refer to carbon (C), hydrogen (H), oxygen (O), nitrogen (N), and sulfur (S).

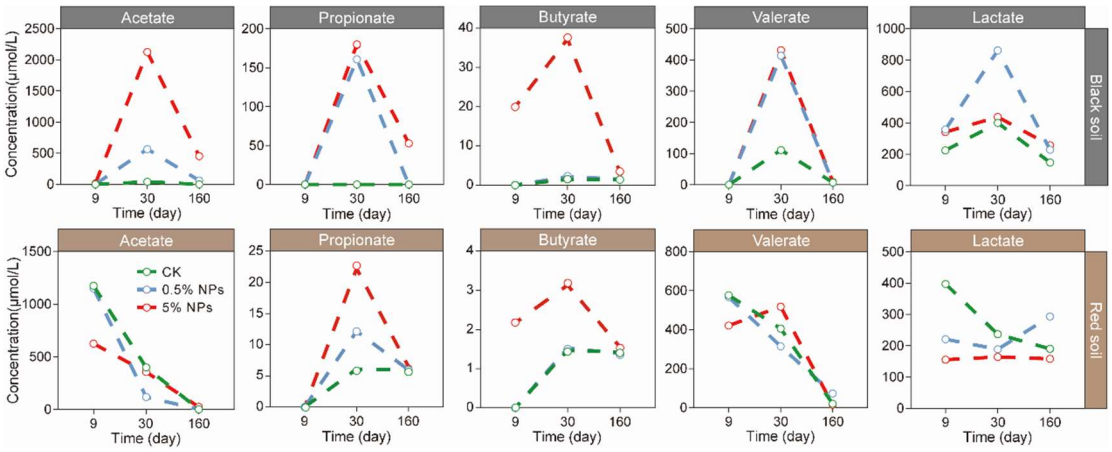

Fig. S5 Concentration of short-chain fatty acids in black and red soils. Acetate, propionate, butyrate, valerate, and lactate were determined after the microcosm incubations for 9 days, 30 days, and 160 days.

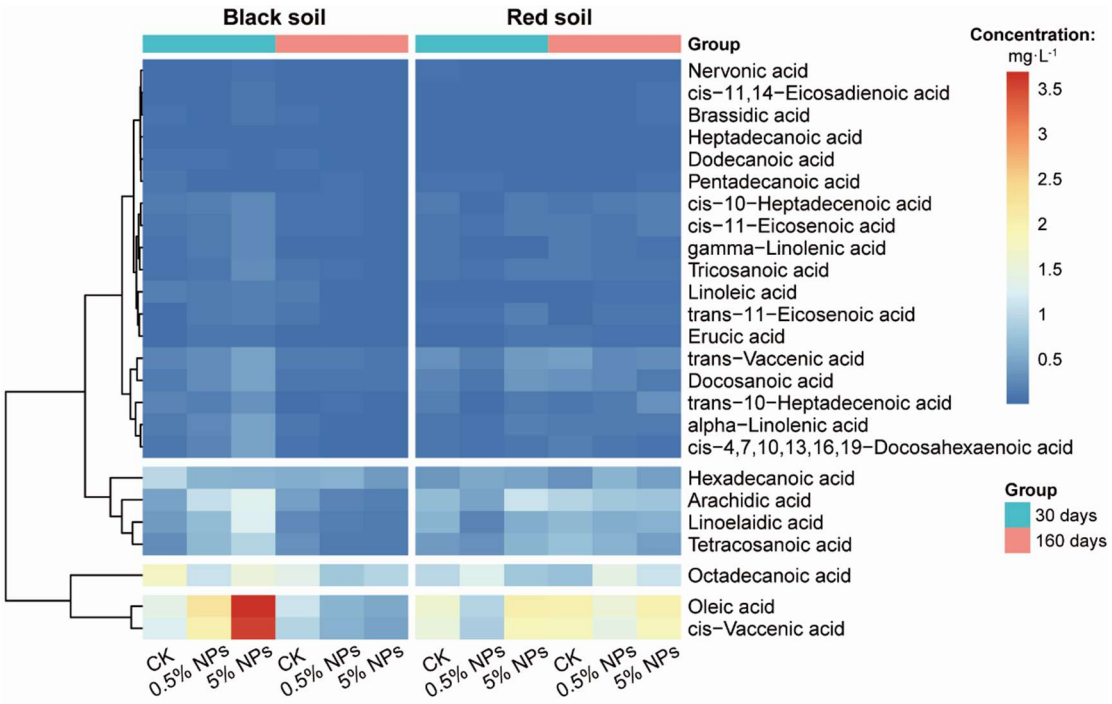

Fig. S6 Concentration of long-chain fatty acids in black and red soils after the microcosm incubations for 30 days and 160 days.

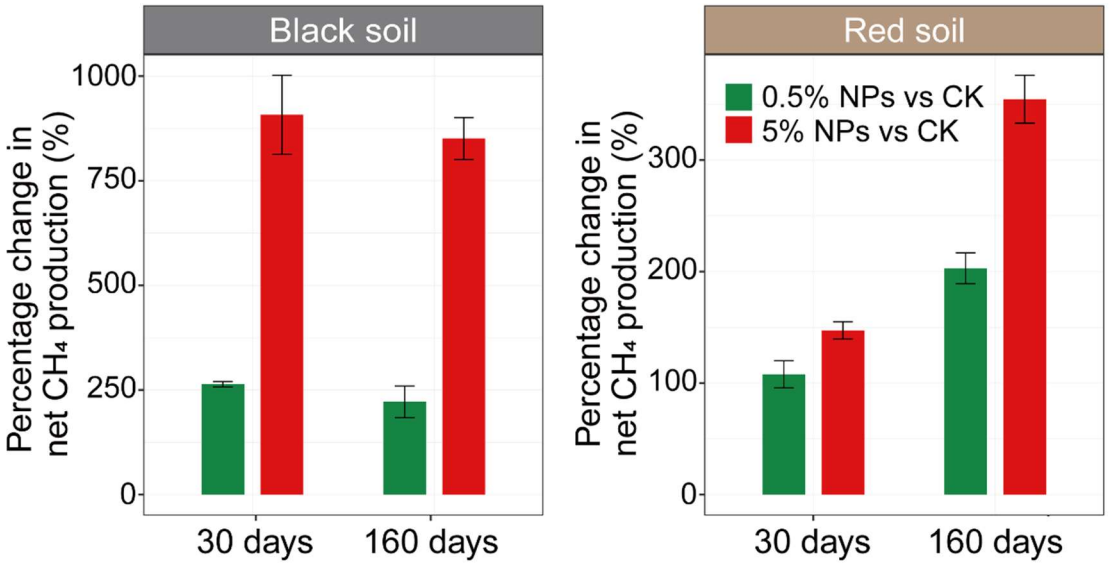

Fig. S7 The percentage change in net CH_4 production in NPs-amended microcosms of the black and red soils after the 30-day and 160-day incubation periods. The percentage change in net CH_4 production was calculated in relation to the control treatment (CK).

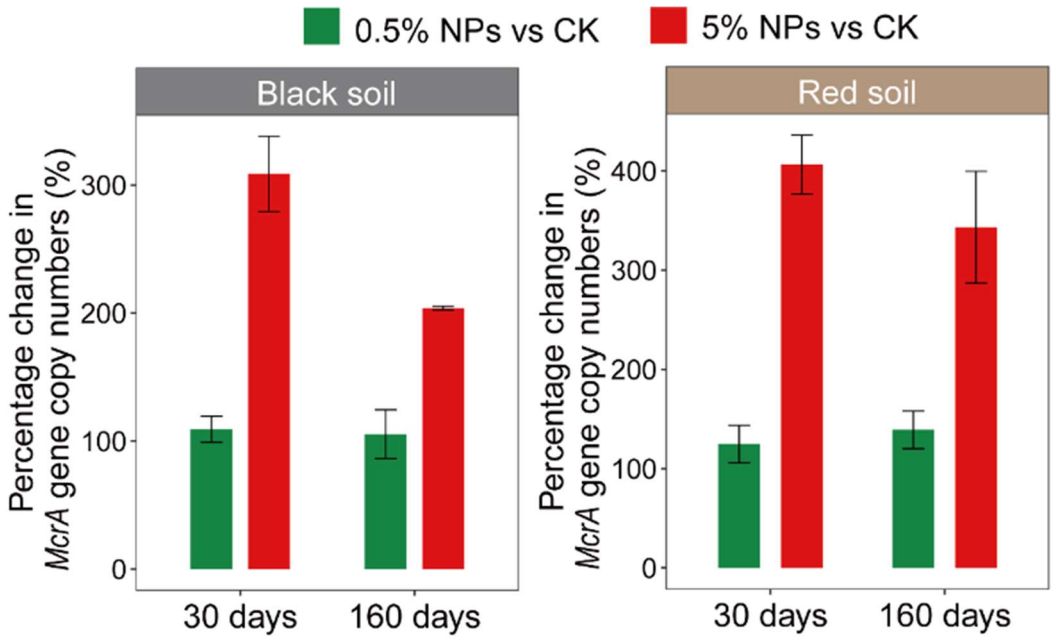

Fig. S8 The percentage change in the *mcrA* gene copy numbers in NPs-amended microcosms of the black and red soils after the 30-day and 160-day incubation periods. The percentage change in *mcrA* gene copy number was calculated in relation to the control treatment (CK).

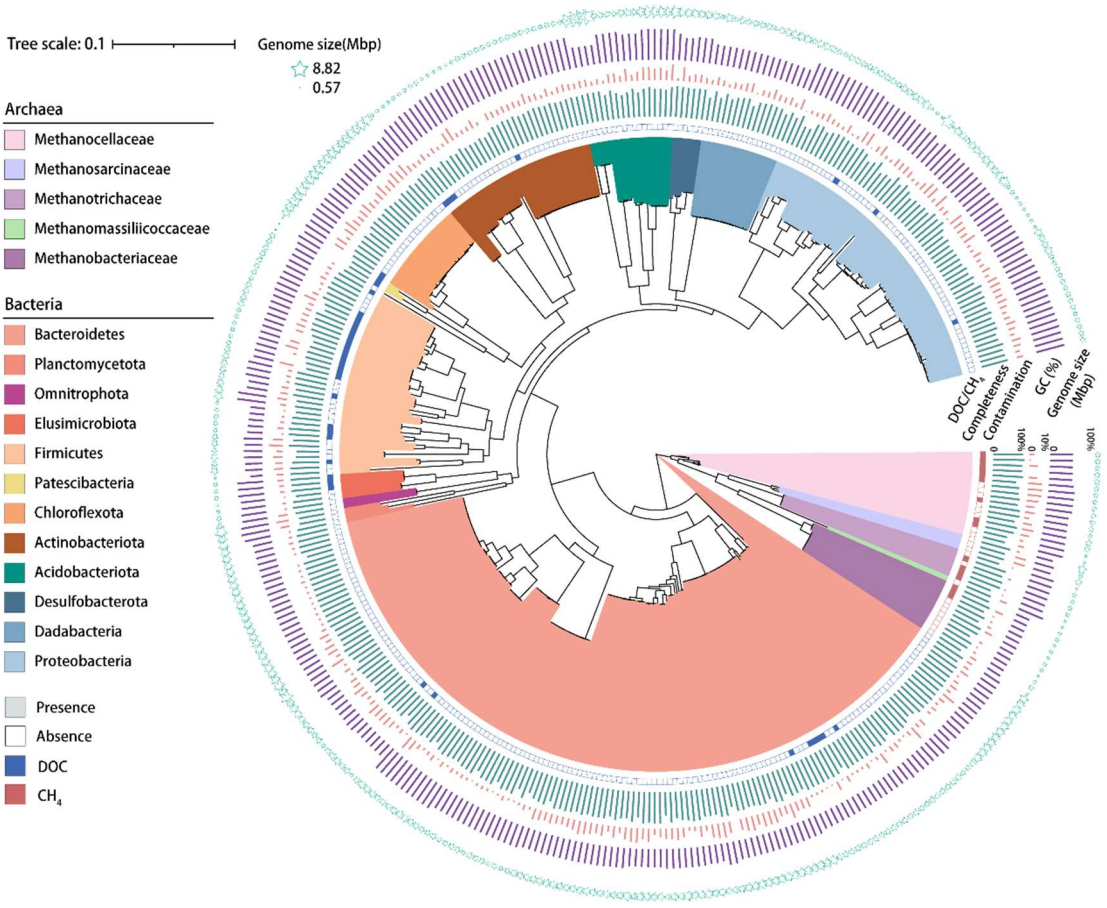

Fig. S9 Phylogenomic trees showing the taxonomic relatedness of all 391 bacterial and methanogen MAGs. While the taxonomic affiliations of the 353 bacterial MAGs are shown at the phylum level, those of the 38 methanogen MAGs are indicated at the family level. The solid boxes in the most inner circle indicate bacterial and methanogen MAGs whose metagenomic abundance is significantly correlated to DOC (blue boxes) and CH_4 (red boxes). Three strip charts indicate the completeness, contamination, and GC (%) of each MAG. The asterisk(s) in the most outer circle represent genome size.

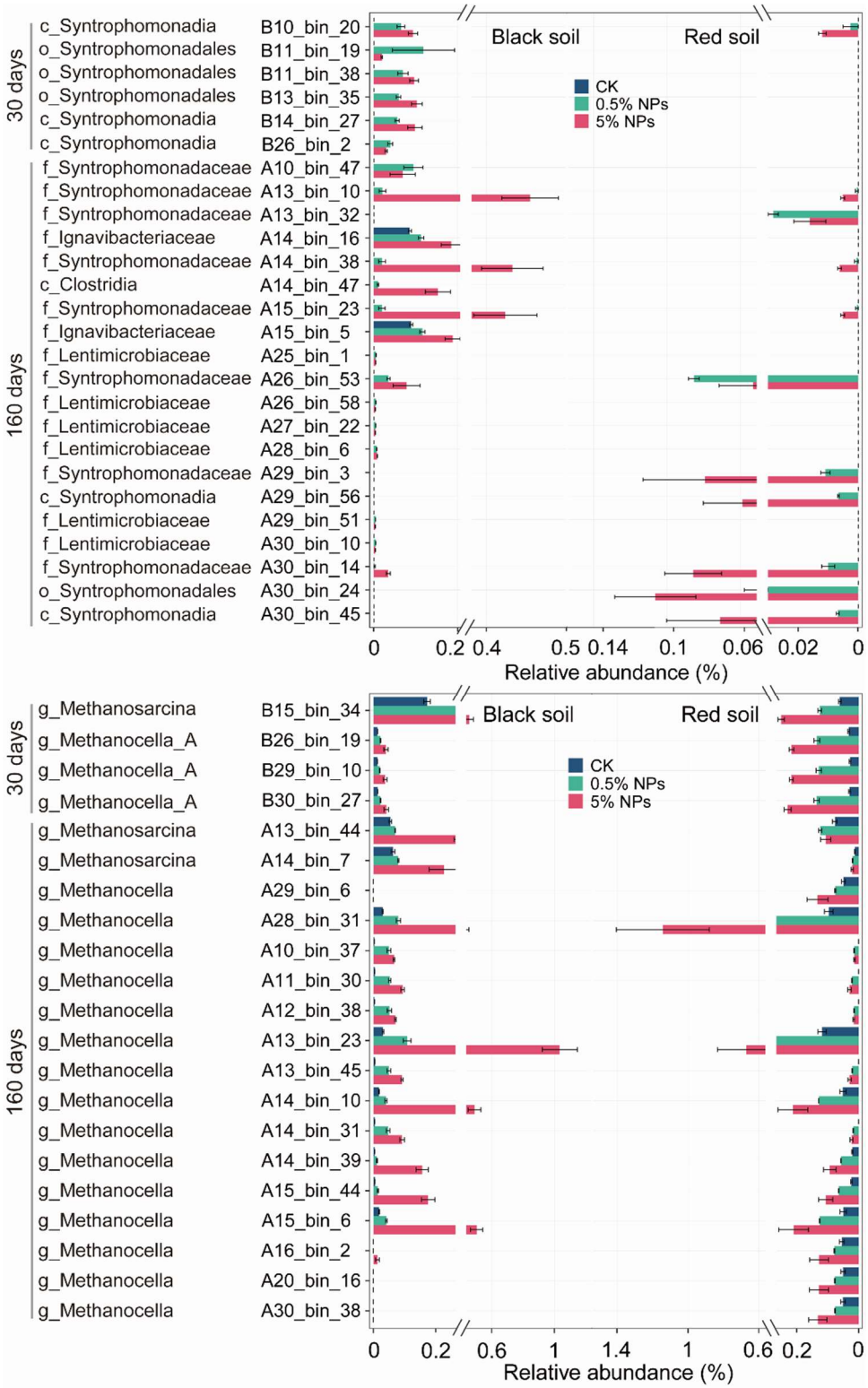

Fig. S10 Representative MAGs that were recovered from black and red soils and exhibited significant changes in their metagenomic abundance between the different treatments (CK, 0.5% NPs, and 5% NPs).

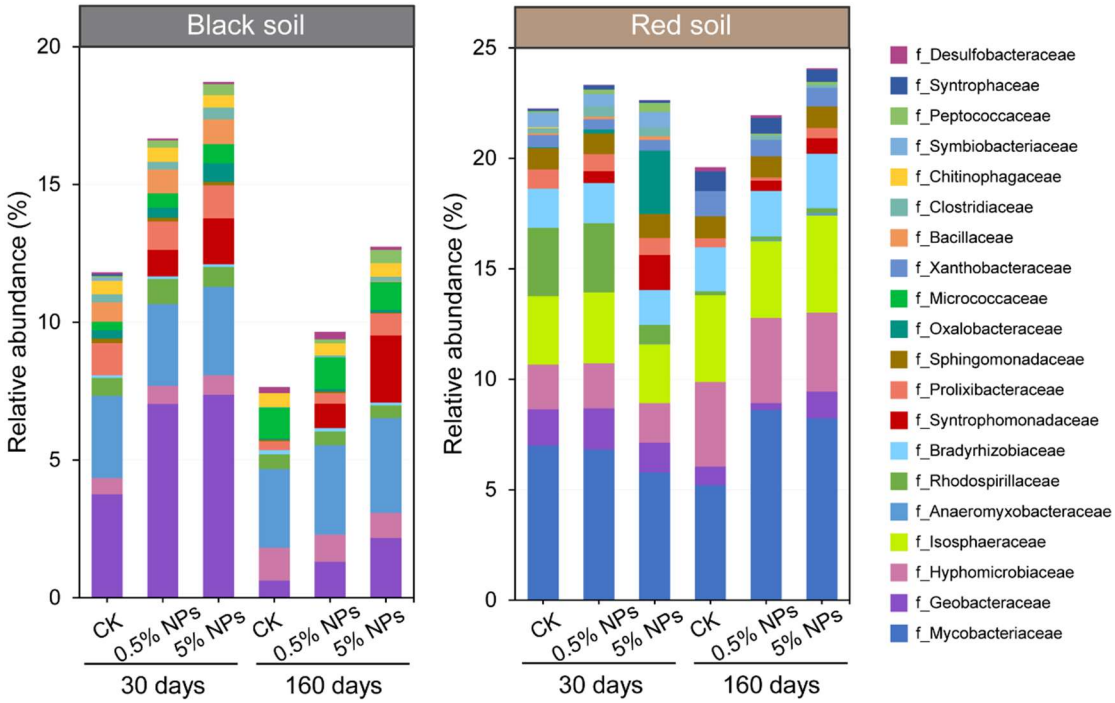

Fig. S11 The 20 most abundant bacterial families in the metagenomes of the control (CK) and LDPE NPs treatments (0.5%, 5%) in the black and red soils after the 30-day and 160-day incubation periods.

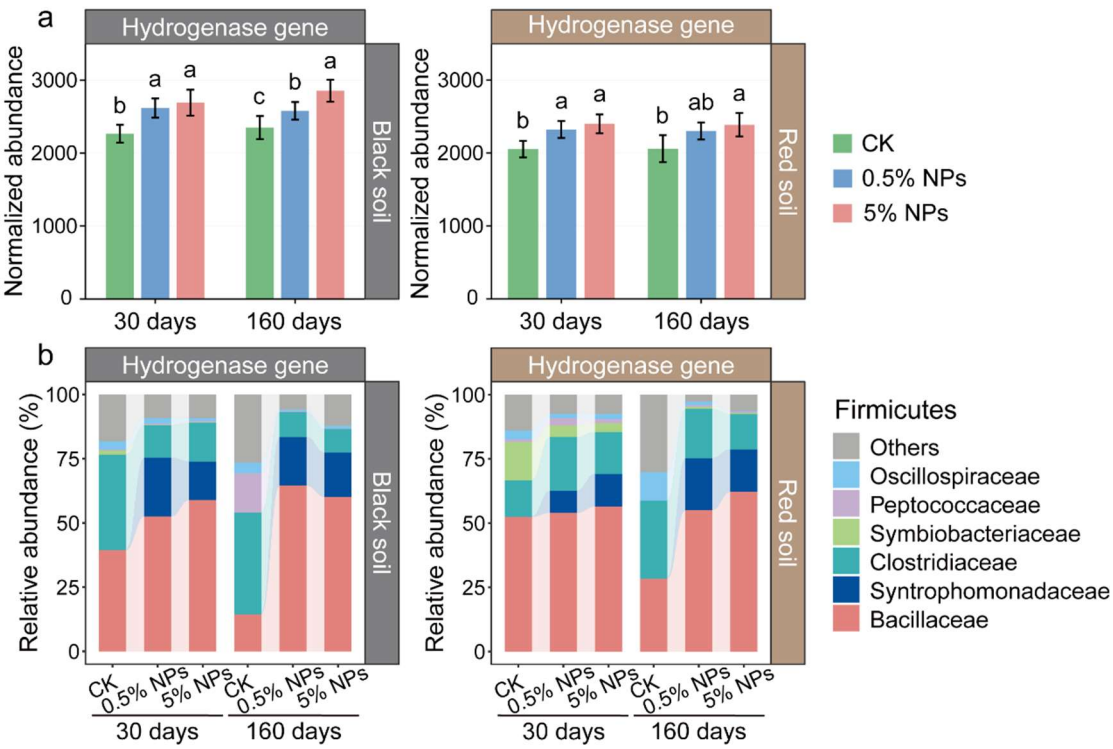

Fig. S12 The normalized abundance and the taxonomic assignment of H_2-evolving hydrogenase genes in the black soil and red soil metagenomes obtained from the control (CK) and LDPE NPs (0.5%, 5%) treatments after the 30-day and 160-day incubation periods. (a) Letters (a,b,c) indicate significant difference in the metagenomic abundance of the H_2-evolving hydrogenase genes between the treatments. Error bars denote standard deviation (n=3). (b) The taxonomic assignment of the H_2-evolving hydrogenase genes was achieved by extracting their sequences from the metagenomic contigs. The extracted sequences were then blasted against the NCBI's non-redundant protein database using Diamond with default settings.

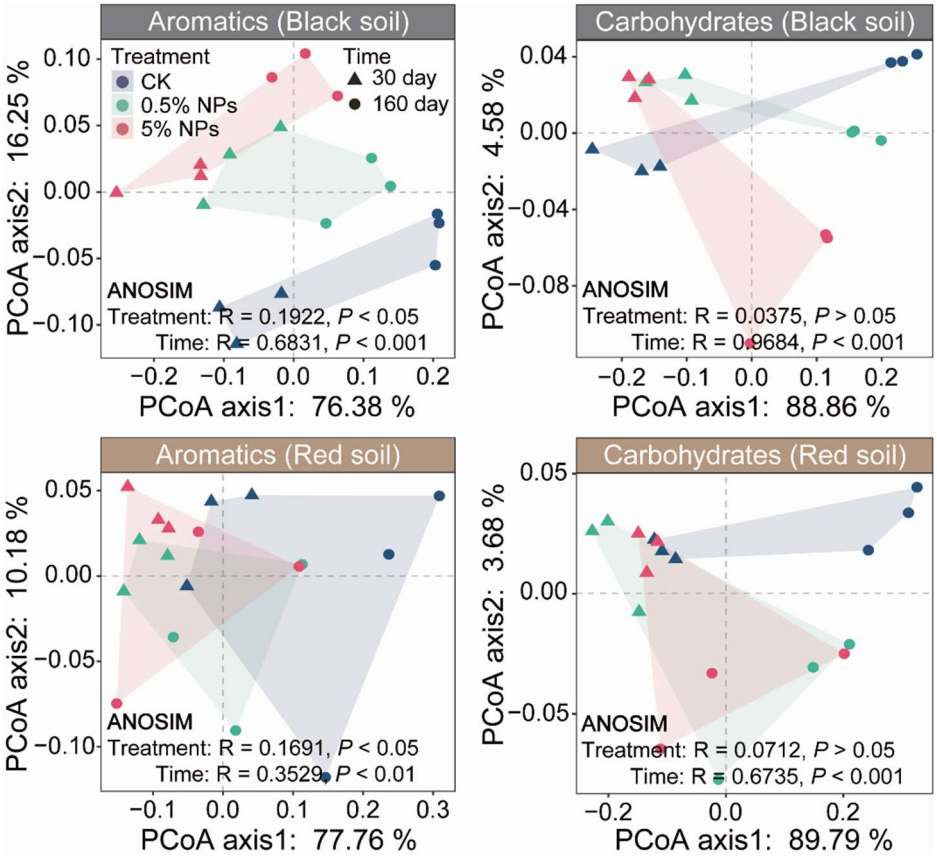

Fig. S13 Principal coordinate analysis (PCoA) of the genes encoding the degradation of aromatics and complex carbohydrates The PCoAs are based on Bray–Curtis distance matrices.

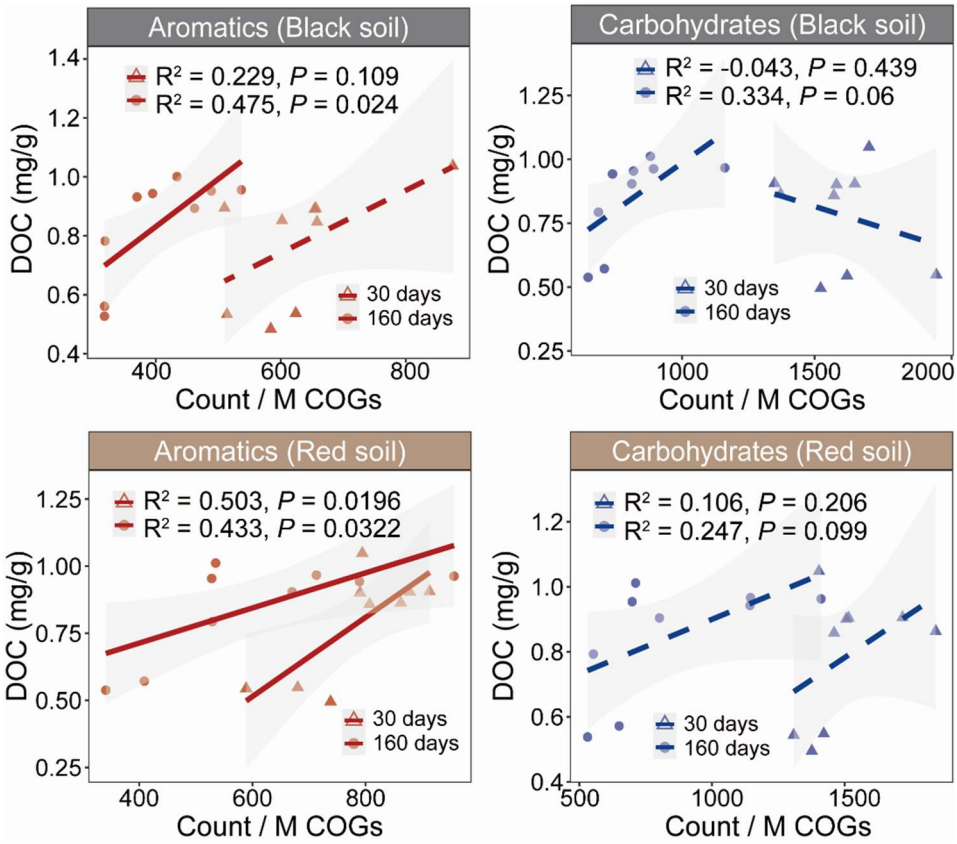

Fig. S14 Treatment-dependent relationship between DOC content and the metagenomic abundance of genes encoding the degradation of aromatics (red lines) and complex carbohydrates (blue lines) in the black and red soils after the 30-day and 160-day incubation periods. Solid lines indicate significance ($P < 0.05$) of the Pearson's correlations, while dashed lines denote non-significance ($P > 0.05$).

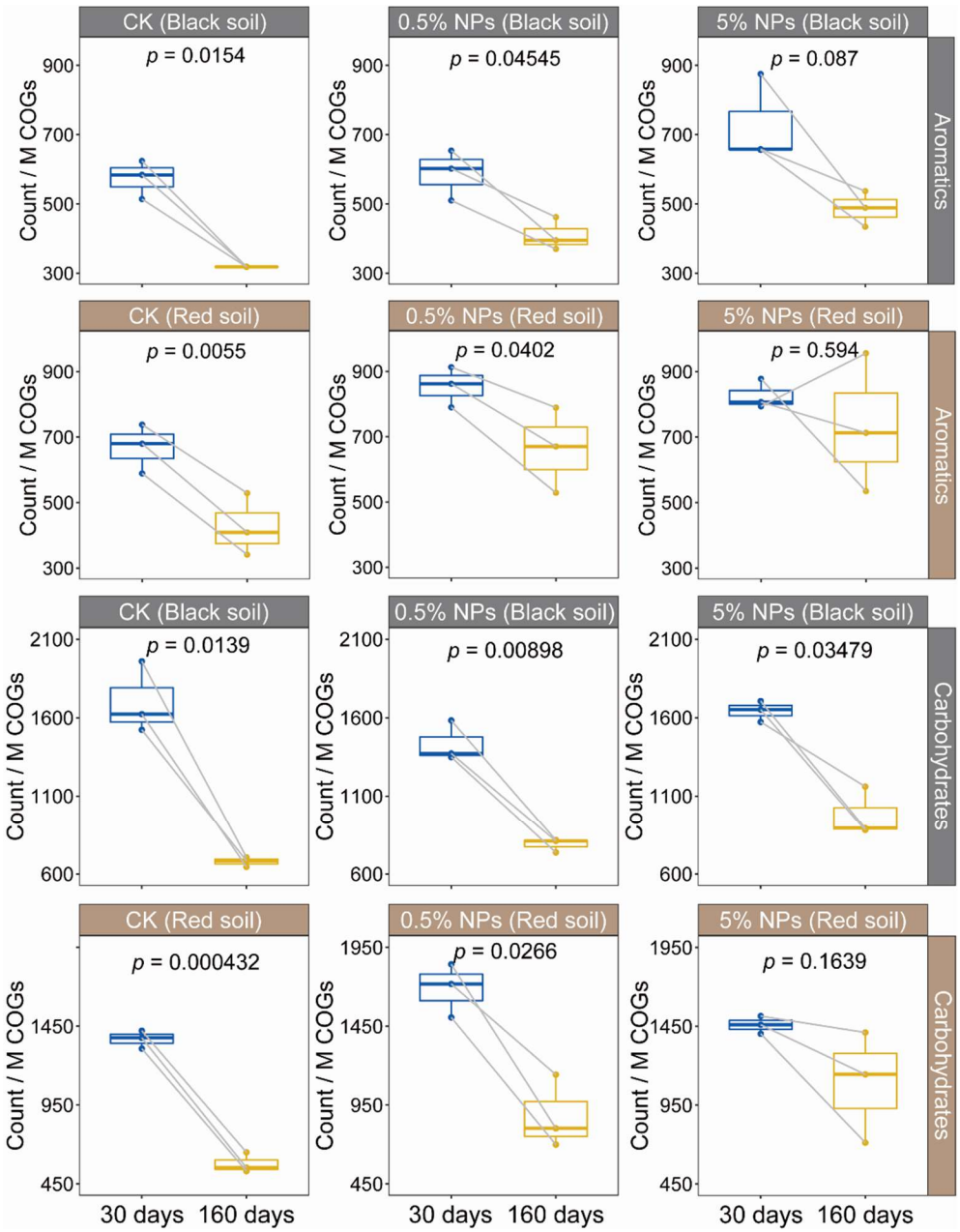

Fig. S15 Change in the metagenomic abundance of genes involved in the degradation of aromatics and complex carbohydrates between the 30-day and 160-day incubation periods. The relative abundance changes between the two incubation times and their significance is shown for each treatment (CK, 0.5% NP, and 5% NP) and soil type. The abundance changes are indicated in counts per million COGs.

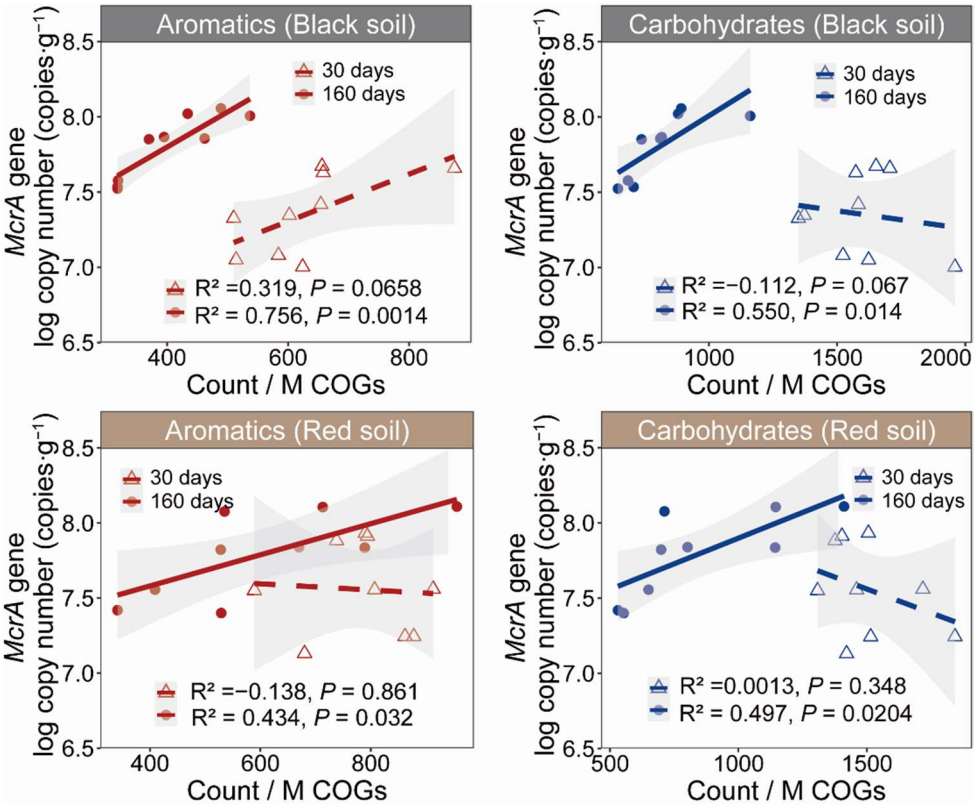

Fig. S16 Treatment-dependent relationship between the *mcrA* gene copy number and the metagenomic abundance of genes encoding the degradation of aromatics (red lines) and complex carbohydrates (blue lines) in black and red soils after the 30-day and 160-day incubation periods. Solid lines indicate significance ($P < 0.05$) of the Pearson's correlations, while dashed lines denote non-significance ($P > 0.05$).

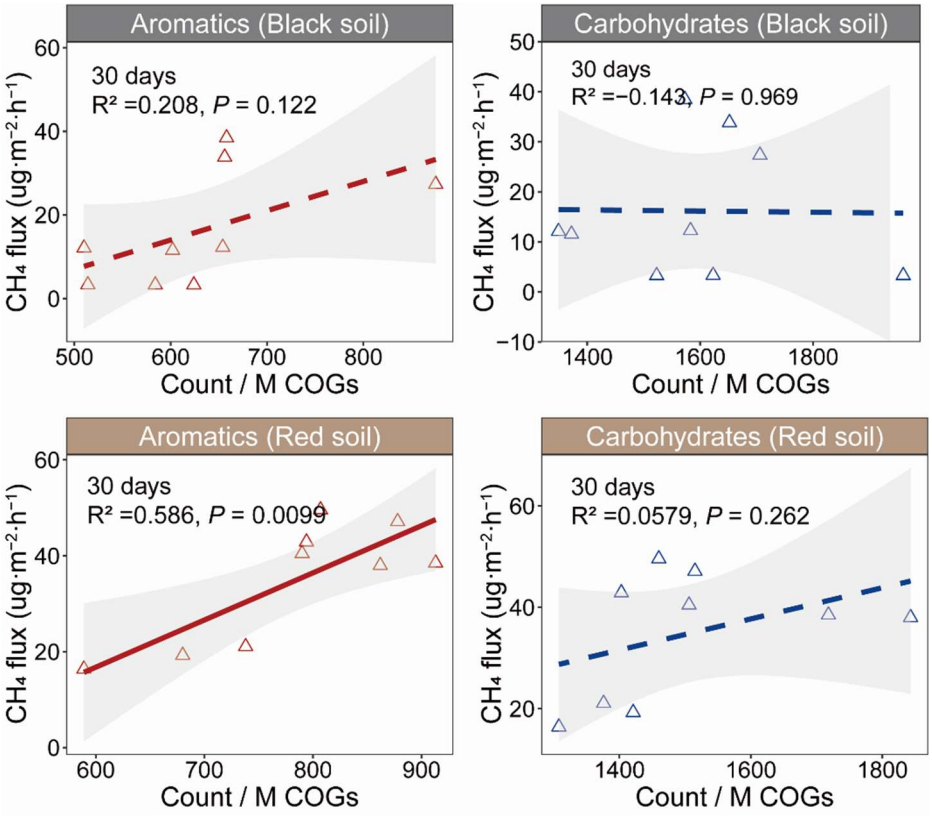

Fig. S17 Treatment-specific relationship between the CH_4 production and the metagenomic abundance of genes encoding the degradation of aromatics and complex carbohydrates in the black and red soils after 30-day incubation. The metagenomic abundance is indicated as counts per million COGs. Solid lines indicate significance ($P < 0.05$) of the Pearson's correlations, and dashed lines denote non-significance ($P > 0.05$).

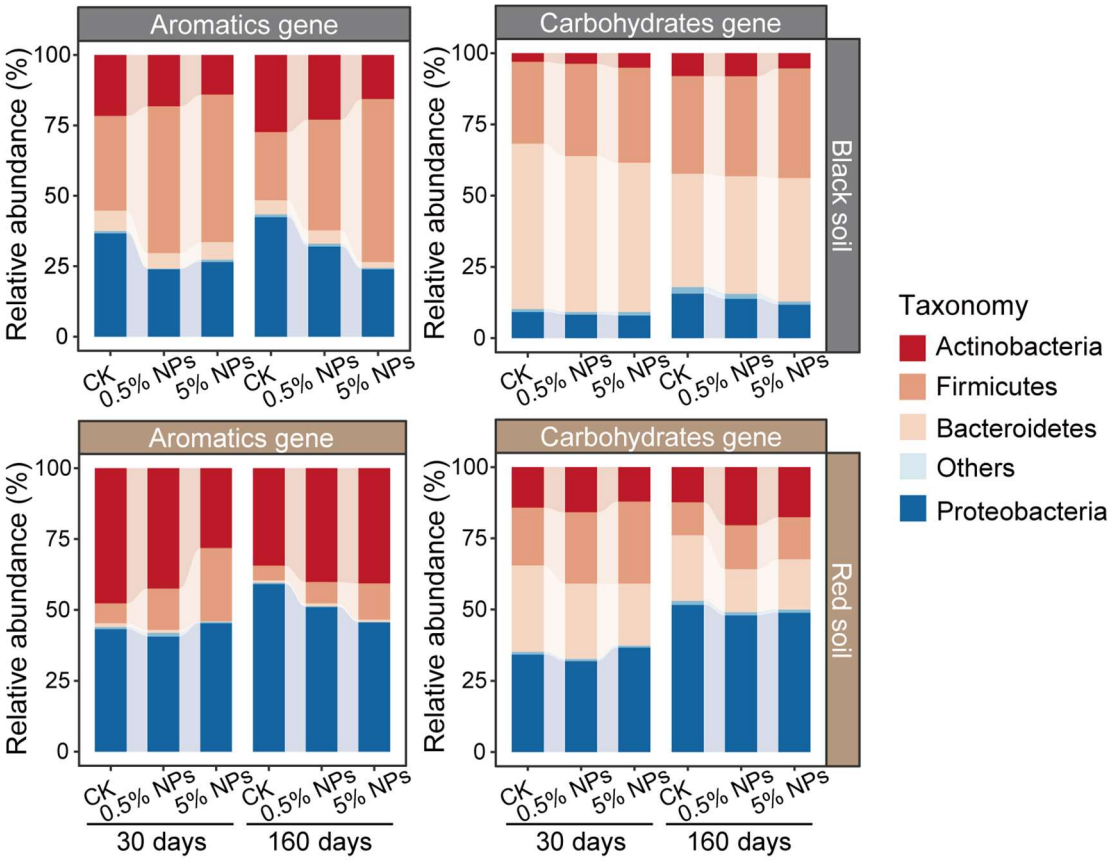

Fig. S18 The bar plots display the phylum-level assignment of genes encoding the degradation of aromatics and complex carbohydrates. Data represents means of three replicates.

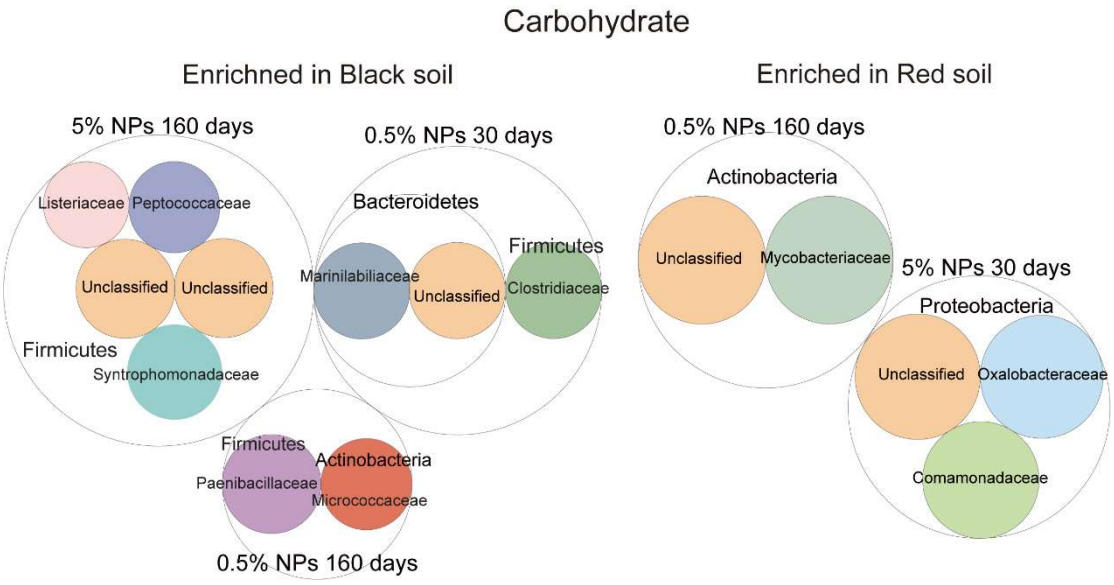

Fig. S19 Circle chart showing the set of genes involved in the degradation of complex carbohydrates and affiliated with bacterial families that, according to LEFse analysis, were specifically enriched in the LDPE nanoplastics treatments (relative to CK) of the black soil or the red soil after the 30-day and 160-day incubation periods. The family-level composition is colored-coded. Circle size is proportional to the relative taxon-specific metagenomic abundance.

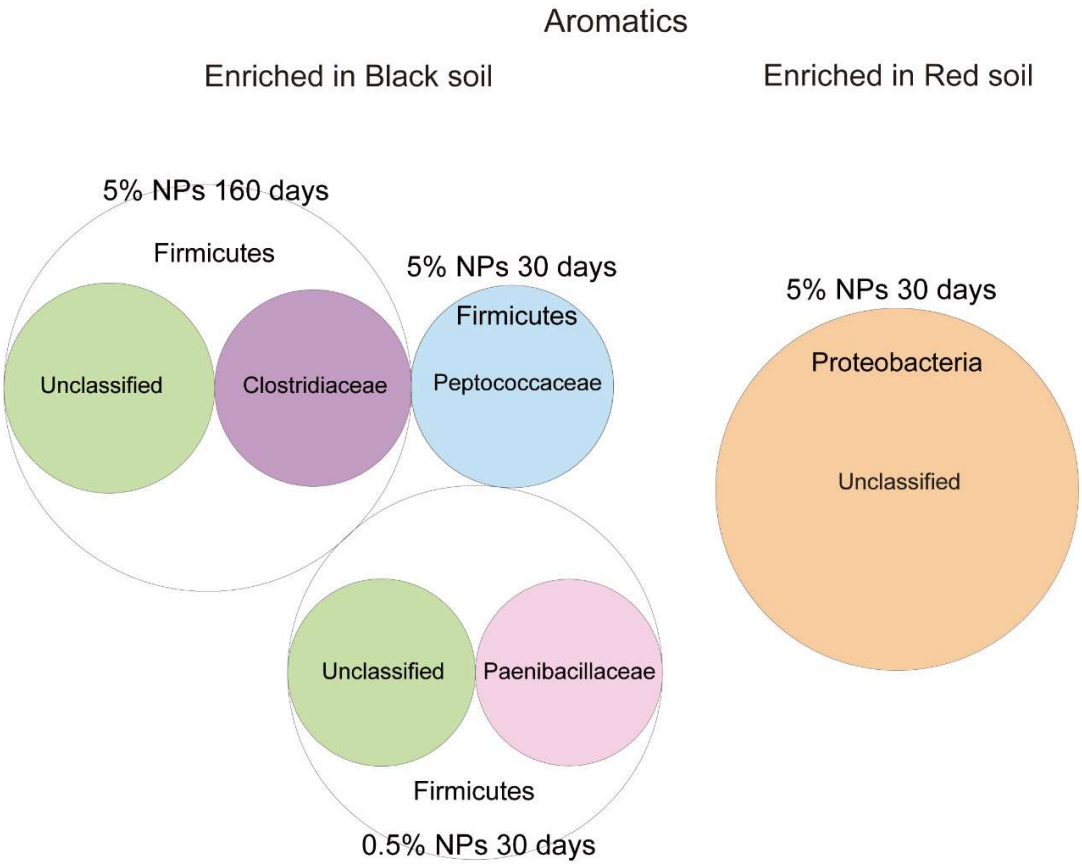

Fig. S20 Circle chart showing the set of genes involved in the degradation of aromatics and affiliated with bacterial families that, according to LEFse analysis, were specifically enriched in the LDPE nanoplastics treatments (relative to CK) of the black soil or the red soil after the 30-day and 160-day incubation periods. The family-level composition is colored-coded. Circle size is proportional to the relative taxon-specific metagenomic abundance.

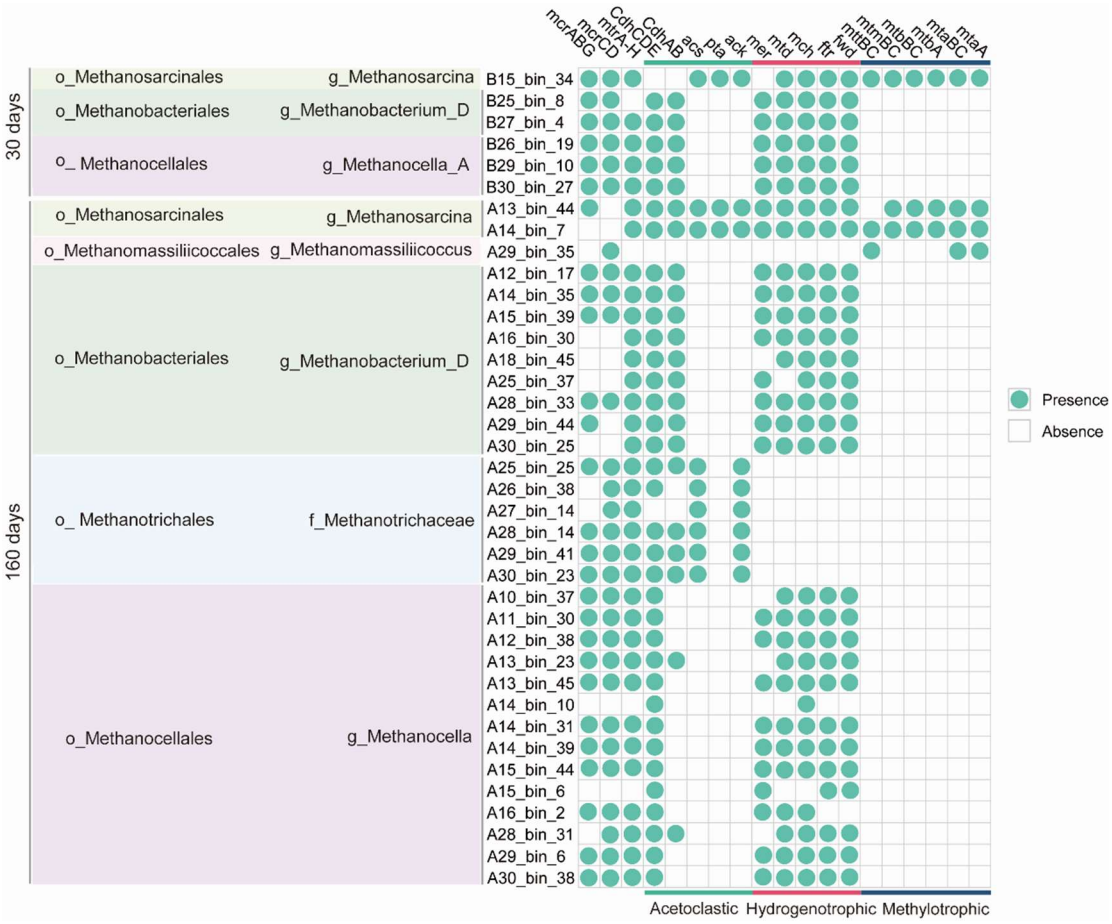

Fig. S21 Heatmap showing the presence of genes encoding particular methanogenic pathways in the 38 methanogen MAGs that were recovered from the LDPE nanoplastics treatments after the 30-day and 160-day incubation periods. The genes and gene clusters represent either common biomarkers for the methanogenic potential or are grouped according to the following pathways: acetoclastic, hydrogenotrophic, and methylotrophic methanogenesis.

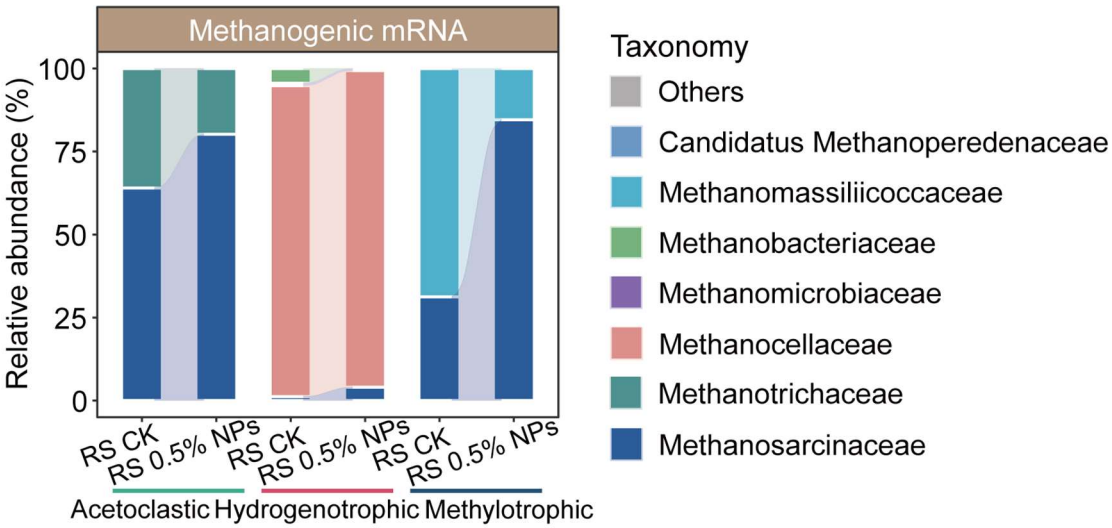

Fig. S22 Taxonomic assignment of mRNA that is highly specific for the acetoclastic, hydrogenotrophic, or methylotrophic methanogenesis pathway. The mRNA was obtained from the control and 0.5% NPs treatments of the red soil after the 160-day incubation period. The mRNA analysis is based on a composite sample (n = 3).

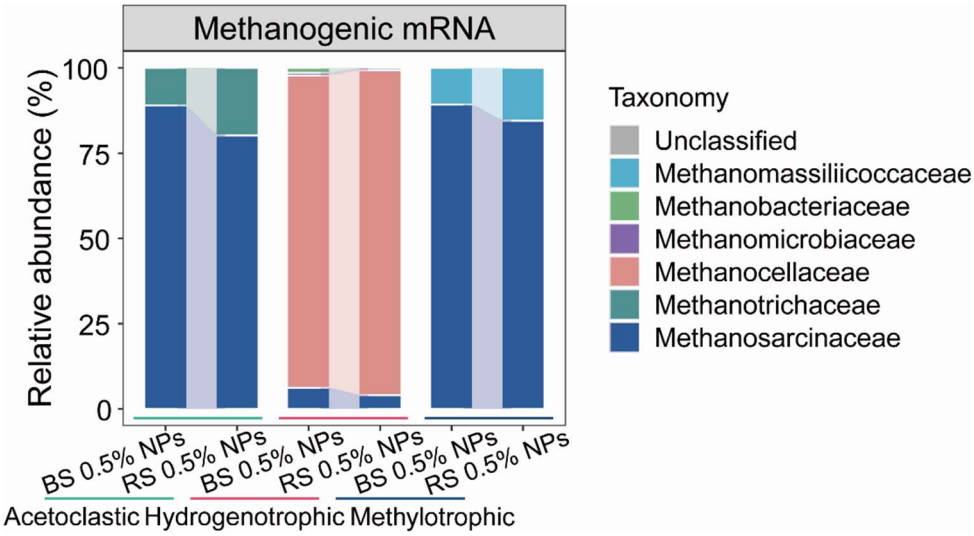

Fig. S23 Family-level comparison of metatranscriptomic mRNA obtained from the 0.5% NPs treatments of the black soil (BS) and the red soil (RS) after the 160-day incubation period. The mRNA is grouped according to the following pathways: acetoclastic, hydrogenotrophic, and methylotrophic methanogenesis.

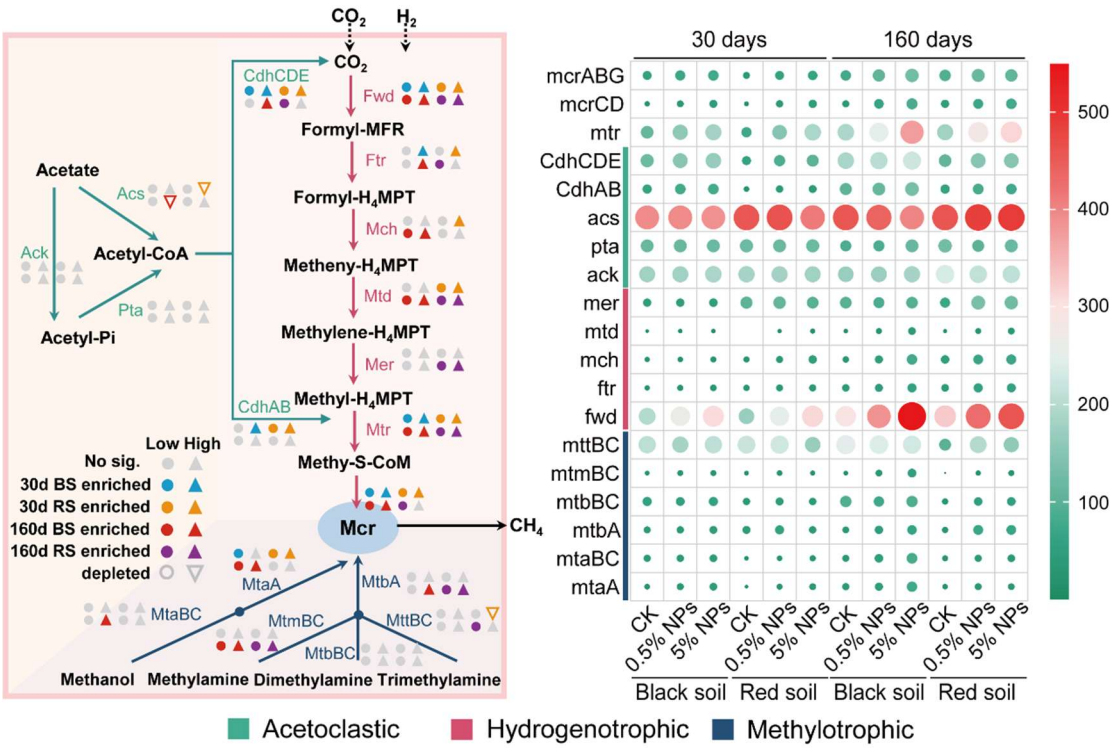

Fig. S24 Metagenomic abundance of genes encoding methanogenesis in the control (CK) and LDPE nanoplastics (0.5%, 5%) treatments of the black and red soils after an incubation period of 30 and 160 days. Schematic presentation of low or high changes in the metagenomic abundance of genes associated with the acetoclastic, hydrogenotrophic, or methylotrophic methanogenesis pathways (left panel). The magnitude of the abundance changes is indicated for each gene across the different treatments by circle size (right panel).

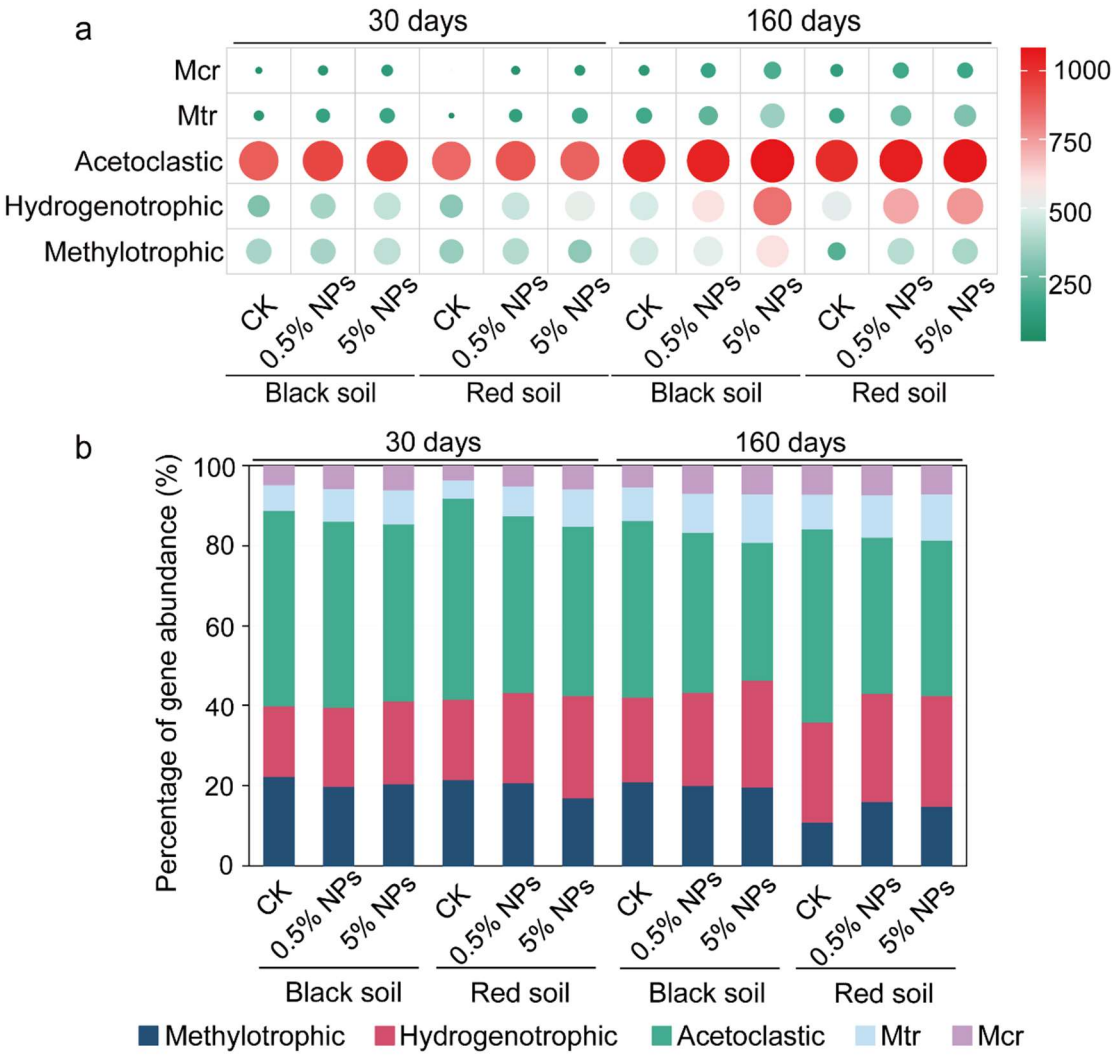

Fig. S25 Collective metagenomic abundance of genes highly indicative of (i) acetoclastic, (ii) hydrogenotrophic, or (iii) methylotrophic methanogenesis in the control (CK) and LDPE nanoplastics (0.5%, 5%) treatments of the black and red soils after the 30-day and 160-day incubation periods. The abundance of common methanogenic marker genes (*mcrA*, *mtr*) is shown separately. (a) The data are shown as relative abundances in the format of a heatmap plot. (b) The data are shown as metagenomic abundances in the format of bar graphs. The collective abundance of genes highly specific for the three methanogenic pathways, along with the relative abundance of *mcr* and *mtr* genes, was set to 100%.

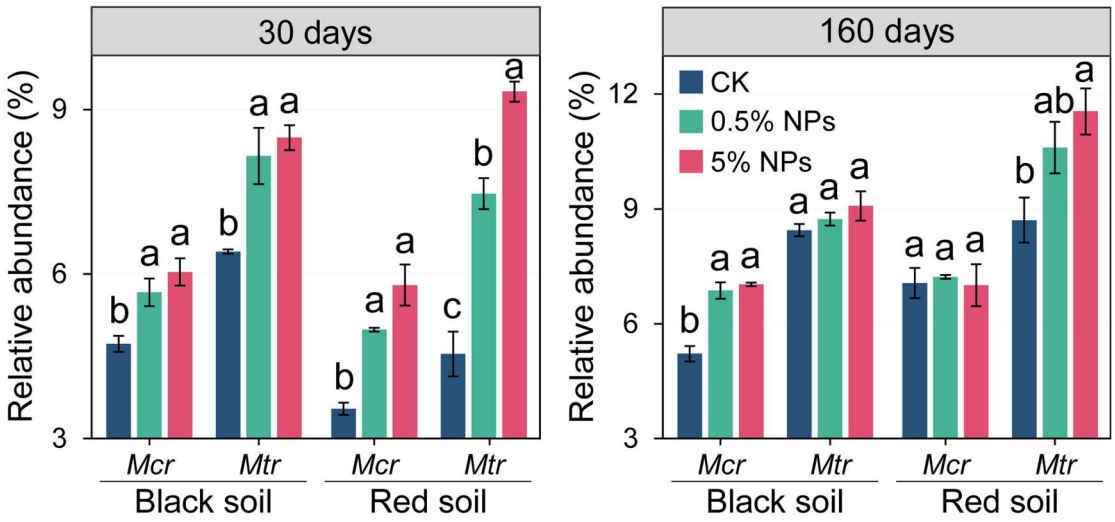

Fig. S26 Changes in the metagenomic abundance of the *mcr* and *mtr* genes in the control (CK) and LDPE nanoplastics (0.5%, 5%) treatments of the black and red soils after the 30-day and 160-day incubation periods. The bar charts are based on the same datasets as shown in Fig. 6. The cumulative relative abundance of the *mcr* and *mtr* genes, along with the relative abundance of the genes encoding the three methanogenesis pathways as shown in Fig. 6, collectively account for 100%. Error bars denote standard deviation (n = 3). The relative abundance of *mcr* and *mtr* genes was calculated based on counts per million reads.

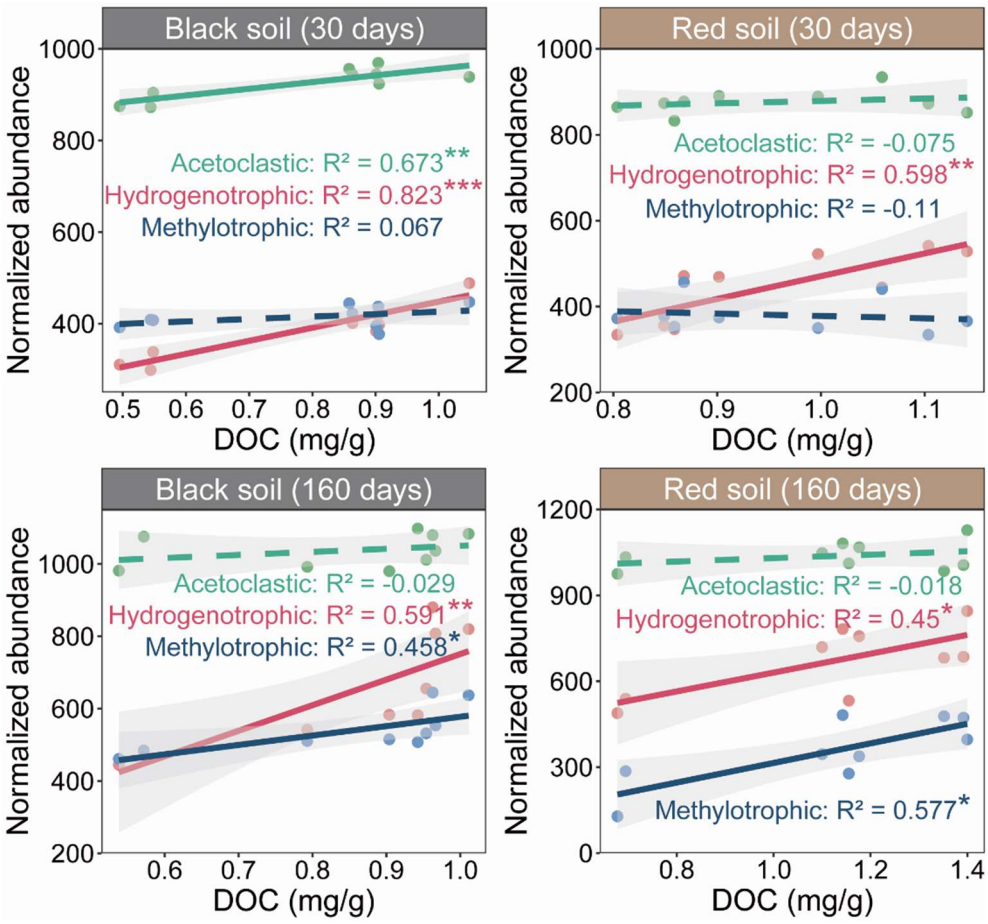

Fig. S27 Linear relationships between the DOC content and the normalized collective metagenomic abundance of genes (counts per million reads) highly indicative of the acetoclastic, hydrogenotrophic, or methylotrophic pathway in the black and red soils after the 30-day and 160-day incubation periods.

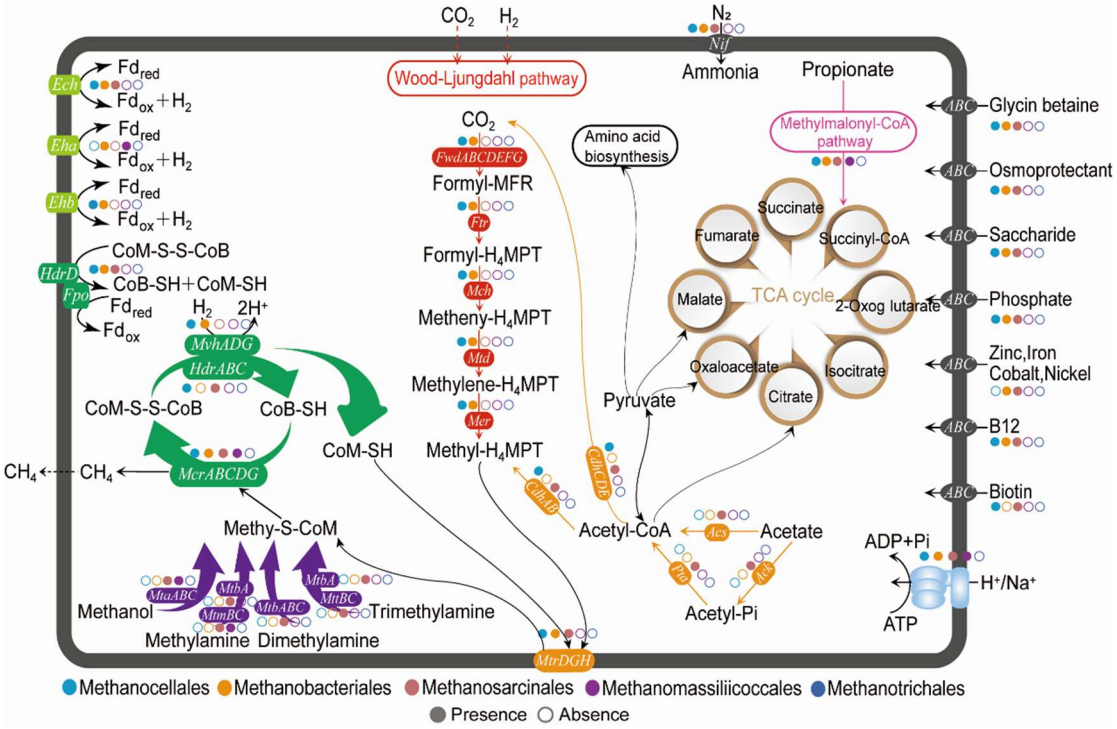

Fig. S28 Metabolic pathways expressed in the five order-level methanogen lineages based on the mapping of metatranscriptomic mRNA to the 38 methanogen MAGs obtained in the course of this study. The expression analysis involved energy conservation and ABC transporter, as well as the carbon, nitrogen, and sulfate metabolism.

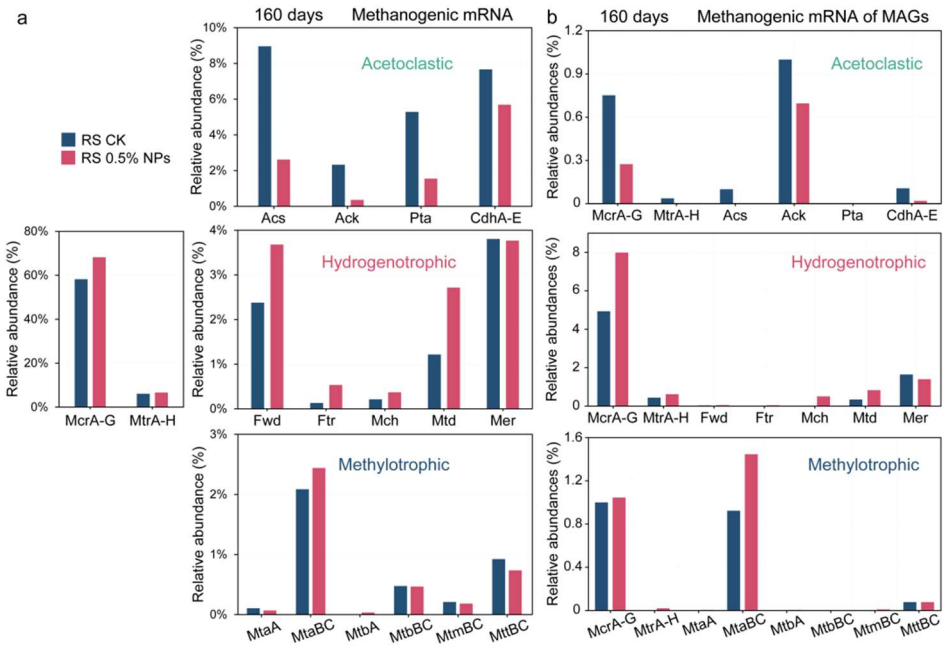

Fig. S29 Bar graphs showing the relative pathway-specific abundances of transcripts encoding acetoclastic, hydrogenotrophic, or methylotrophic methanogenesis in the metatranscriptomes obtained from the control and 0.5% NPs treatments of the red soil (RS) after the 160-day incubation period. The analysis involved a mapping-independent (direct) mRNA analysis (a) and a mapping-dependent mRNA analysis using 14 methanogen MAGs. Each metatranscriptome was mapped separately. The relative abundances are indicated as percentage of total reads annotated to KEGG level 3 (methane metabolism).

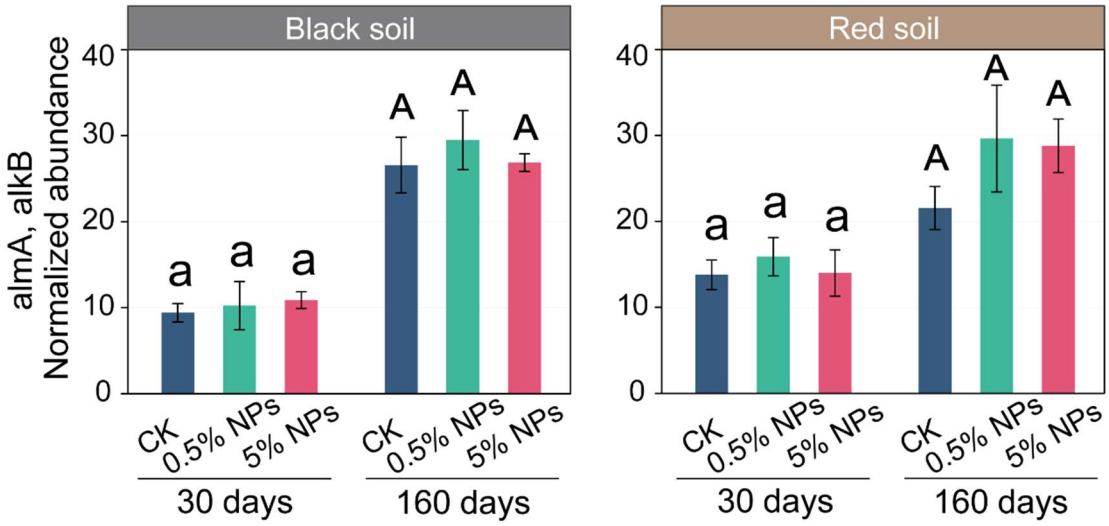

Fig. S30 The normalized metagenomic abundances of the *almA* and *alkB* genes (counts per million reads) in the control (CK) and LDPE NPs (0.5%, 5%) treatments of the black and red soils after the 30-day and 160-day incubation periods.

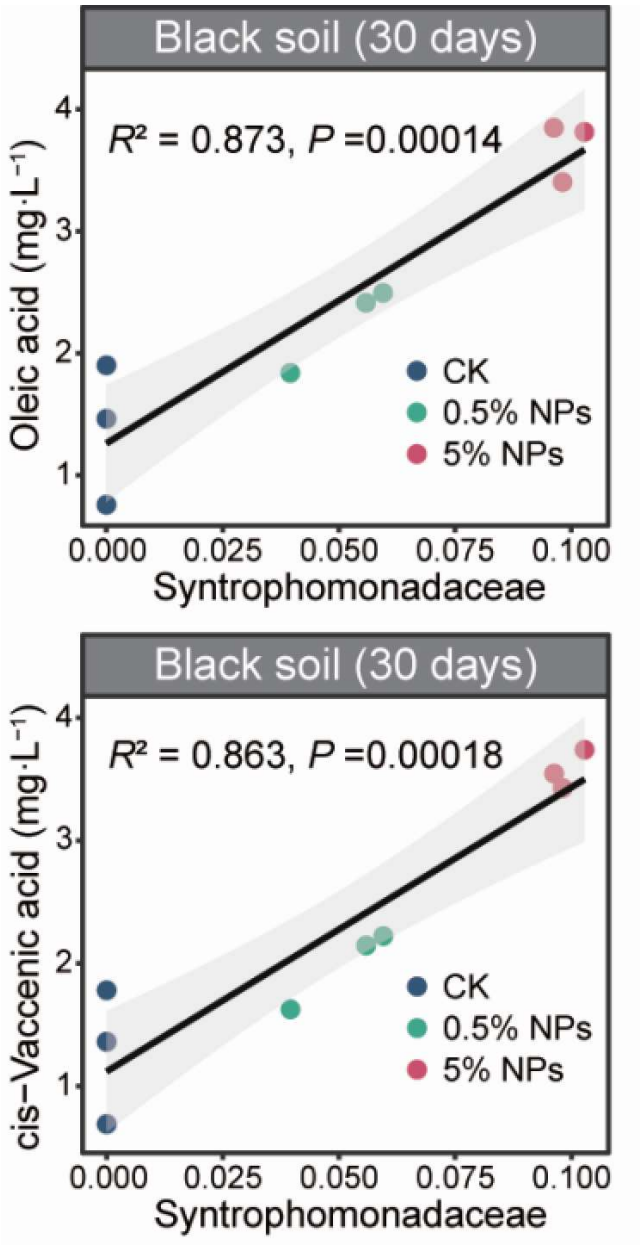

Fig. S31 Correlations between the metagenomic abundance of Syntrophomonadaceae and the concentrations of oleic acid and cis-vaccenic acid across the control (CK) and LDPE NPs (0.5%, 5%) treatments of the black soil after the 30-day and 160-day incubation periods.